Journal of Power Sources 325 (2016) 620–629

Contents lists available at ScienceDirect

Journal of Power Sources

journal homepage: www.elsevier.com/locate/jpowsour

A facile cathode design combining Ni-rich layered oxides with Li-rich layered oxides for lithium-ion batteries

Bohang Song [a], Wangda Li [a], Pengfei Yan [b], Seung-Min Oh [a], Chong-Min Wang [b], Arumugam Manthiram [a, *]

[a] Materials Science and Engineering Program & Texas Materials Institute, The University of Texas at Austin, Austin, TX 78712, USA
[b] Environmental Molecular Science Laboratory, Pacific Northwest National Laboratory, 902 Battelle Boulevard, Richland, WA 99352, USA

HIGHLIGHTS

- A cathode material combining Ni-rich and Li-rich phase was developed.
- The existence of Li-rich phase improves the surface chemical stability.
- Li-rich ordering is observed in layered oxide with Ni-rich ($x > 0.5$) rather than Mn-rich ($y > 0.5$).
- Excellent cycle performance is achieved in both half and pouch-type full cell.

GRAPHICAL ABSTRACT

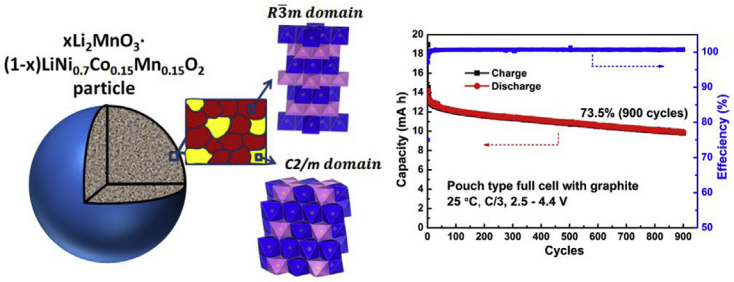

ARTICLE INFO

Article history:
Received 7 March 2016
Received in revised form
23 May 2016
Accepted 13 June 2016

Keywords:
Nickel-rich layered oxide
Lithium-rich layered oxide
Surface chemical stability
Pouch-type full cell

ABSTRACT

A facile synthesis method has been developed to prepare $xLi_2MnO_3 \cdot (1-x)LiNi_{0.7}Co_{0.15}Mn_{0.15}O_2$ ($x = 0$, 0.03, 0.07, 0.10, 0.20, and 0.30) cathode materials, combining the advantages of the high specific capacity of the Ni-rich layered phase and the surface chemical stability of the Li-rich layered phase. X-ray diffraction (XRD), transmission electron microscopy (TEM), and electrochemical charge/discharge measurements confirm the formation of a Li-rich layered phase with $C2/m$ symmetry. The high-angle annular dark-field (HAADF) scanning transmission electron microscopy (STEM) reveals a spatial relationship that the Li-rich nano-domain islands are integrated into the conventional Ni-rich layered matrix ($R\bar{3}m$). Most importantly, this is the first time that Li-rich phase has been directly observed inside a particle at the nano-scale, when the overall composition of the layered oxide $Li_{1+\delta}Ni_{1-y-z-\delta}Mn_yM_zO_2$ (M = metal) is Ni-rich (>0.5) rather than Mn-rich (>0.5). Remarkably, the $xLi_2MnO_3 \cdot (1-x)LiNi_{0.7}Co_{0.15}Mn_{0.15}O_2$ cathodes with optimized x value shows superior electrochemical performance at C/3 rate: an initial capacity of 190 mA h g^{-1} with 90% capacity retention after 400 cycles in a half cell and 73.5% capacity retention after 900 cycles in a pouch-type full cell.

1. Introduction

The demand for high-energy-density power sources is rapidly increasing for applications ranging from small portable electronic devices to large systems such as electric vehicles and smart grids. Currently, the highest energy density provided by the state-of-the-

* Corresponding author.
E-mail address: manth@austin.utexas.edu (A. Manthiram).

http://dx.doi.org/10.1016/j.jpowsour.2016.06.056
0378-7753/

art commercial lithium-ion batteries is ~160 W h kg^{-1}. Therefore, new electrode materials capable of delivering higher energy densities with long cycle life and better thermal stability are necessary for next-generation batteries. Among the known cathode candidates, the layered structure generally offers high theoretical (~270 mA h g^{-1}) compared to the other competitors such as spinel (140 mA h g^{-1}) and olivine (170 mA h g^{-1}) systems [1,2]. Unfortunately, only 50% of Li^+ ions could be reversibly extracted from the currently used layered $Li_{1-x}CoO_2$, resulting in a reduction in the energy density of the commercialized $LiCoO_2$/graphite cells.

To explore an alternative, the co-substitution of Ni and Mn at the Co sites in $LiCoO_2$ produces a family of $LiCo_{1-y-z}Ni_yMn_zO_2$ cathodes. The three ions play different roles in determination of the electrochemical properties of $LiCo_{1-y-z}Ni_yMn_zO_2$: Ni as an electron supplier, Co for sustaining an ordering of layered structure, and Mn for good chemical stability [3]. In this regard, Ni-rich layered oxides $LiNi_{1-y-z}Mn_yCo_zO_2$ with Ni content $(1-y-z) > 0.5$ is drawing worldwide interest in recent years [4–9]. Sun's group [10] has summarized the different roles of Ni, Co, and Mn in the $LiNi_{1-y-z}Mn_yCo_zO_2$ system when Ni content exceeds 1/3, in terms of specific capacity, cycle life, and thermal stability. It is important to note that although the Ni-rich cathodes are capable of delivering a 180–210 mA h g^{-1} capacity when $0.6 < x < 0.9$, the capacity retention and thermal stability are sacrificed with increasing Ni content. Poor capacity retention is believed to be associated with undesirable side reactions between the tetravalent transition metal ions, in particular Ni^{4+}, and the electrolyte [11,12] and phase transition from layered to rock-salt structure (NiO) at particle's surface [13], both of which cause a substantial decline in the lithiation kinetics at the electrode-electrolyte interphase. On the other hand, poor thermal stability arises due to the release of oxygen from the crystal lattice at the highly delithiated state [8,14]. Finding out the most suitable composition to meet the industry demands for overall performance remains a challenge to battery researchers.

As for another family of promising cathode candidates, the Li-rich layered oxides, denoted as $xLi_2MnO_3\cdot(1-x)LiNi_aCo_bMn_cO_2$ $(a + b + c = 1)$ have also gained extensive attention due to their even higher reversible capacities of more than 250 mA h g^{-1} [15,16]. One of the signatures for these materials is that Li^+ ions partially reside at the transition-metal layer sites in the local lattice, where the Mn^{4+}-rich environment around the Li^+ ions form a supperlattice arrangement with a special $C2/m$ symmetry. Upon charging, Li^+ ion extraction involves a release of oxygen from the lattice, leading to structural instability and inevitable rearrangement of residual Li^+ and transition-metal ions to form a thermodynamically-favorable spinel phase [17–19]. The layered to spinel transformation causes a voltage decay, resulting in a gradual loss of output energy density upon cycling. The voltage decay is recognized as the main issue hindering the practical application of the Li-rich layered oxide cathodes. Although spinel transformation is inevitable, the Li-rich layered oxide cathodes commonly show enhanced cyclability even though the charge cut-off voltage is relatively high (~4.6 V). Such enhanced cyclability is ascribed to the less reactivity of Mn^{4+} with the electrolyte that minimizes the decline of lithiation kinetics at the electrode-electrolyte interphase and the less formation of Jahn-Teller Mn^{3+} ions in the host lattice [20,21]. In summary, the Ni-rich layered oxides deliver stable voltage profile with reasonable specific capacity but suffer from surface chemical instability, whereas the Li-rich layered oxides exhibit reasonably good surface chemical stability but suffer from voltage-decay upon cycling.

Inspired by the individual advantages and disadvantages of the Ni-rich and Li-rich layered oxide cathodes, here we report a novel $xLi_2MnO_3\cdot(1-x)LiNi_{0.7}Co_{0.15}Mn_{0.15}O_2$ ($x = 0$, 0.03, 0.07, 0.10, 0.20, and 0.30 as molar ratio) layered oxide cathodes prepared by a facile method. The idea is to integrate a small amount of Li-rich phase into the Ni-rich phase to stabilize the Ni-rich phase from chemical corrosion, while avoiding the use of a large amount of Li-rich phase minimizes the voltage decay effect. As a result, the modified cathode materials show superior electrochemical performance compared to the conventional Ni-rich layered $LiNi_{0.7}Co_{0.15}Mn_{0.15}O_2$ oxide both at room and elevated temperatures. Li et al. [9] recently reported the synthesis of a core-shell structure with a Ni-rich composition as a core and a Li-rich composition as a shell to improve the performance. Choi et al. [22] also reported a smart compositional design of $(1-x)Li(Ni_{0.95}Co_{0.05})O_2\cdot xLi_2MnO_3$ ($x = 0.05$ and 0.1) to achieve Li-rich features inside the Ni-rich particles. Here in our case, for the first time, structural investigation with high-angle annular dark-field (HAADF) scanning transmission electron microscopy (STEM) shows a clear evidence of $C2/m$ nano-domains embedded in the $R\bar{3}m$ lattice for such high-Ni content layered oxides.

2. Experimental

2.1. Synthesis of $xLi_2MnO_3\cdot(1-x)LiNi_{0.7}Co_{0.15}Mn_{0.15}O_2$

$Ni_{0.7}Co_{0.15}Mn_{0.15}(OH)_2$ precursor was prepared by a transition-metal hydroxide co-precipitation method with a continuous stirring tank reactor (CSTR). Prior to the precipitation reaction, a desired amount of saturated NH_4OH was added to the CSTR for the establishment of the initial condition. Subsequently, a metal solution containing $NiSO_4\cdot6H_2O$, $CoSO_4\cdot7H_2O$, and $MnSO_4\cdot H_2O$ with a molar ratio of 70: 15: 15 at a combined concentration of 1.0 M was fed into the CSTR at a controlled rate. In the meantime, 2.0–4.0 M KOH aqueous solution with NH_4OH was pumped separately into the CSTR to maintain the pH value within the appropriate range (~11) during the reaction, along with N_2 as a protective gas. Throughout the co-precipitation process, the amount of NH_4OH added and the temperature (50 °C) were also carefully monitored and controlled. After filtering, washing, and drying at around 100 °C under vacuum overnight, the as-synthesized precursor particles were collected. To prepare the various $xLi_2MnO_3\cdot(1-x)LiNi_{0.7}Co_{0.15}Mn_{0.15}O_2$ ($x = 0$, 0.03, 0.07, 0.10, 0.20, and 0.30 as molar ratios) samples, 2 g of the $Ni_{0.7}Co_{0.15}Mn_{0.15}(OH)_2$ precursor was mixed and ground with a certain amount of $MnCO_3$ (calculated based on the required amount of Li_2MnO_3) and corresponding amount of $LiOH\cdot H_2O$ (with 3% excess) for 10 min. Subsequently, the mixture was preheated at 500 °C for 12 h before heating up to 800 °C for 15 h, and then quenched in liquid nitrogen.

2.2. Structural characterization

The chemical compositions were determined by inductively coupled plasma optical emission spectroscopy (ICP-OES, Varian 715 ES). Powder X-ray diffraction (XRD) analysis was carried out with a Rigaku Miniflex 600 in a 2θ range of 10°–80° with a scan speed of 1° per min with Cu Kα radiation. Lattice parameters and weight ratios of the two phases were further revealed by Rietveld refinement based on the General Structure Analysis Software (GSAS) [23]. Particle morphology and energy dispersive X-ray (EDX) elemental mapping were characterized by scanning electron microscopy (SEM, FEI Quanta 650). As-prepared cathode powders were dusted on carbon grids for transmission electron microscopy (TEM). A probe Cs-corrector scanning/TEM microscope (FEI Titan™ 80–300 operated at 300 kV) was used for high angle annular dark filed (HAADF) imaging and EDX analysis. Under the STEM mode, the electron beam had a convergence angle of 17.8 mrad and HAADF signal was collected by the annular detector in the range of 55–220 mrad. Another FEI Titan™ 80–300 microscope with image